

PCCP

Accepted Manuscript



This is an *Accepted Manuscript*, which has been through the Royal Society of Chemistry peer review process and has been accepted for publication.

Accepted Manuscripts are published online shortly after acceptance, before technical editing, formatting and proof reading. Using this free service, authors can make their results available to the community, in citable form, before we publish the edited article. We will replace this *Accepted Manuscript* with the edited and formatted *Advance Article* as soon as it is available.

You can find more information about *Accepted Manuscripts* in the [Information for Authors](#).

Please note that technical editing may introduce minor changes to the text and/or graphics, which may alter content. The journal's standard [Terms & Conditions](#) and the [Ethical guidelines](#) still apply. In no event shall the Royal Society of Chemistry be held responsible for any errors or omissions in this *Accepted Manuscript* or any consequences arising from the use of any information it contains.



Journal Name

ARTICLE

Effect of Meta Coupling on Colour Purity, Quantum Yield, and Excitons Utilizing Efficiency in Deep-Blue Emitters from Phenanthroimidazole Isomers

Received 00th January 20xx,
Accepted 00th January 20xx

DOI: 10.1039/x0xx00000x

www.rsc.org/

Zhiming Wang^{*ad}, Xueying Li^a, Wanyu Zhang^a, Shitong Zhang^b, Hui Li^a, Zhenqiang Yu^d, Yanming Chen^a, Ping Lu^b, Ping Chen^{*c}

Meta-coupling isomers usually exhibit bluer emission than do the *para*-isomers, but the loss of efficiency with respect to photoluminescence (PL) and electroluminescence (EL) is an inevitable result in most cases, particularly for deep blue emitters. In this study, three blue emitting isomers, 4,4'-bis(1-phenyl-phenanthro[9,10-d]imidazol-2-yl)biphenyl (BPPI), 3,4'-bis(1-phenyl-phenanthro[9,10-d]imidazol-2-yl)biphenyl (L-BPPI) and 3,3'-bis(1-phenyl-phenanthro[9,10-d]imidazol-2-yl)biphenyl (Z-BPPI), were chosen as model compounds to investigate the essential reason behind the *meta*-coupling effect due to their different coupling forms, viz. *para-para*, *para-meta*, and *meta-meta*, respectively, in similar dimeric phenanthroimidazole frameworks. A combination of detailed photophysical data, device performance and DFT calculations for the excited state provided valuable information. In particular, the relationship between certain key parameters in calculations as well as PL or EL properties was confirmed, such as oscillator strength and quantum yield, among others, which could effectively reduce the issues related to synthesis and characterisation using prior computer simulations. Good agreement was observed in the results obtained from calculation and experiments, and it was concluded that *meta*-tuning barely realised improvement in EL, unless some special excited states formed or excitons conversion channel appeared, as in the case of reverse intersystem crossing.

1. Introduction

During the past decades, organic deep-blue light-emitting materials have attracted considerable attention because of their characteristics such as effective reduction of power consumption and increase in the colour gamut of full-colour organic light-emitting diodes (OLEDs).^{1,2} They can also be utilized as hosts for generating green, red or white light by energy transfer to a suitable emissive dopant.^{3,4} As criteria for evaluating the performance of different blue or deep-blue emitters for OLEDs, the three most important and widely accepted indexes are as follows: colour purity (CP), quantum yield (QY) and external quantum efficiency (EQE) or excitons utilizing efficiency (EUE).⁵

As a guarantee, CP is typically employed as a key parameter to

represent the Commission Internationale de l'Éclairage (CIE) coordinates. For example, the criterion for a blue emitter is set as $x + y < 0.30$ by the National Television System Committee (NTSC), while that for a deep (saturated) blue emitter is further limited to $y < 0.08$, which is improved to $y < 0.06$ by the European Broadcasting Union (EBU).⁶ In practical emission spectra, the main peak (λ_{\max}) and full-width at half-maximum (FWHM) play decisive roles in CIEs for blue emitters, of which λ_{\max} can be easily designed and tuned by controlling the molecular structure, such as degree of conjugation, coupling mode and donor (acceptor) moiety intensity, and so on. As a successful strategy for organic fluorescent materials, *meta*-coupling is typically applied instead of *para*-coupling because the *meta*-isomer has significantly bluer emissions than the *para*-one.⁷ However, their corresponding changes in photoluminescence (PL), electroluminescence (EL) and EUEs were mysterious, and in most cases, their corresponding values for the *meta*-isomer decreased as compared to those for the *para*-one. To explain these losses, the weakened induced effect and conjugated effect have been typically employed, but it is imperative for investigate the fundamental reasons behind this loss with the aim of designing high-efficiency materials with good CP.

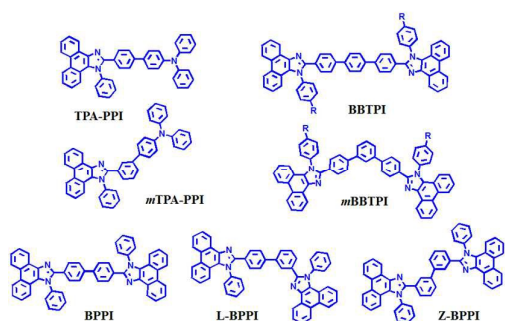
Recently, aryl-substituted phenanthroimidazole (API) has emerged as a building block for the preparation of high-efficiency blue-emitting materials with characteristics such as satisfactory CP,

^a School of Petrochemical Engineering, Shenyang University of Technology, 30 Guanghua Street, Liaoyang, 111003, P. R. China; Fax: +86 419 5319409; Tel: +86 419 5319409; E-mail: wangzhm1983@163.com

^b State Key Laboratory of Supramolecular Structure and Materials, Jilin University, 2699 Qianjin Avenue, Changchun 130012, P.R. China.

^c State Key Laboratory on Integrated Optoelectronics, College of Electronic Science and Engineering, Jilin University, 2699 Qianjin Avenue, Changchun 130012, P.R. China; E-mail: pingchen@jlu.edu.cn

^d Shenzhen Research Institute, The Hong Kong University of Science & Technology, No. 9 Yuexing 1st RD, South Area Hi-tech Park, Nanshan, Shenzhen 518057, China. Electronic Supplementary Information (ESI) available: [details of excited states characters, Lippert-Mataga model and electroluminescence properties]. See DOI: 10.1039/x0xx00000x



Scheme 1. Structures of API derivatives with para- and meta-coupling

excellent thermal properties, high fluorescence QY, potential bipolar properties and high EUE (>25%).⁸⁻¹⁶ In addition, these materials can be synthesised by a simple method. When applying the *meta*-coupling mode instead of the *para*-coupling mode, API-based materials and their OLEDs show obvious blue-shifts in CIEs, and more saturated blue emissions are observed with the loss of QY and EUE (or EQE). For instance, Yang has reported a favourable CIE of (0.15, 0.11) for TPA-PPI and its OLED performance with a good EQE of 5.02%, with a corresponding EUE value of greater than 25% (Scheme 1).^{15a} By tuning the coupling position between TPA and API, *m*TPA-PPI was prepared; more attractive near-ultraviolet emission with CIEs of (0.161, 0.049) was observed, but the QY and EQE decreased to 35% and 3.33%, respectively (The QY of TPA-PPI is 90%).^{15d} A similar observation has been reported by Tong. The CIEs of *amb*BBTPI-based device is located at (0.16, 0.06), which is significantly bluer than the *para*-one (BBTPI) with CIE(0.15, 0.10), but the QY and EQE decrease to 59% and 3.63%, respectively; these values are lower than those (82% and 5.77%) of BBTPI in the same measurements.^{12c} In fact, the aforementioned changes are probably attributed to the tuning of the molecular excited states.

To investigate the possible essential rules of this tuning from *para*-coupling to *meta*-coupling, three isomers, 4,4'-bis(1-phenylphenanthro[9,10-d]imidazol-2-yl)biphenyl (BPPI), 3,4'-bis(1-phenylphenanthro[9,10-d]imidazol-2-yl)biphenyl (L-BPPI) and 3,3'-bis(1-phenylphenanthro[9,10-d]imidazol-2-yl)biphenyl (Z-BPPI), are employed as model compounds because of their gradual coupling from *para-para*, to *para-meta*, to *meta-meta*. In contrast to our previous study on the basic characters and OLED applications of these three isomers, this work focuses on investigating the essential reasons behind tuning and the relationship between the tuning of the meta-isomer and the CP, QY, and EUE or EQE from the changes in their excited-state properties. Combining the density functional theory (DFT) calculation results with the natural transition orbital (NTO) analysis based on the hybridised local and charge-transfer (HLCT) theory, detailed photo-physical data and device performances, some valuable information could be clarified. More importantly, some key parameters could be estimated by DFT calculations, and the PL or EL properties of the meta-isomer are predicted to some degree on the basis of the para-isomer; this approach could effectively mitigate the issues related to synthesis and characterisation using the prior computer simulations. We expect that the results obtained could aid in the design of high-efficiency materials with high EUE and good colour purity for use in non-doped blue OLEDs, avoiding redundant synthesis work and

unnecessary environment pollution during purification of the materials. Some detailed experimental evidence and theoretical analysis are discussed in the following sections.

2. Experimental section

BPPI, L-BPPI and Z-BPPI were prepared according to previously reported studies.^{9c} Their UV-vis absorption spectra were recorded on a UV-3100 spectrophotometer. Fluorescence measurements were carried out using an RF-5301PC system. HPLC-grade solvents used for spectral measurements were purchased from Aldrich or Acros and used without purification.

All density functional theory calculations were carried out using the Gaussian 09 B.01 Package, and geometry optimization was carried out in the gas phase. The ground states of the three isomers were calculated at the B3LYP/6-31G (d, p) level, which is commonly used for precise geometry optimisation.¹⁵ The excited states were calculated at the M06-2X/6-31G (d, p) level; the results obtained were in good agreement with the experimental UV and PL data according to our previous discussion.

Electroluminescence (EL) devices were fabricated by the vacuum deposition of the materials at 10^{-6} Torr onto ITO glass with a sheet resistance of $25 \Omega \text{ square}^{-1}$. All organic layers were deposited at a rate of 1.0 \AA s^{-1} . The cathode was deposited with Mg and Ag at a deposition rate of 0.1 \AA s^{-1} . The EL spectra and CIE coordinates of these devices were measured using a PR650 spectra scan spectrometer. The luminance-current and density-voltage characteristics were recorded simultaneously with the measurement of the EL spectra by combining the spectrometer with a Keithley model 2400 programmable voltage-current source. All measurements were carried out at room temperature under ambient conditions.

3. Results and discussion

3.1 Theoretical Calculations

The basic thermal, photochemical and electro-properties of BPPI, L-BPPI and Z-BPPI were compared and discussed in our previous study (Tab.1).^{9c} As expected, the main emission peaks exhibited obvious blue-shifts, from the *para-para* coupling form (BPPI) to the *para-meta* (L-BPPI) and *meta-meta* forms (Z-BPPI) in the solution

Table 1 Thermal and photophysical data of BPPI, L-BPPI and Z-BPPI

	T_g (°C)	T_d^a (°C)	PL ^b / Φ_{fl}^c λ_{max} (nm) (soln)	PL ^d / Φ_{fl} λ_{max} (nm) (film)	E_{gap}^e (eV)
BPPI	195	535	421/0.92	468/0.85	3.18
L-BPPI	178	542	411/0.68	434/0.57	3.15
Z-BPPI	166	486	368/0.55	402/0.35	3.30

a. Temperature at 5% weight loss of the oligomers; b. Maximum peak in solution; c. Fluorescence quantum yield in solution compared to a 0.5 M H_2SO_4 solution of quinine as the reference (0.54); d. Film thickness is 50 nm; e. Solid-state quantum yield was measured using an integrating sphere apparatus using Alq₃ as the reference (0.22); e. Band gaps were calculated from electrochemistry data using the energy level of the ferrocene (Fc) as the reference (4.8 eV) and calibrated using $E_{1/2}(\text{Fc}/\text{Fc}^+)$.

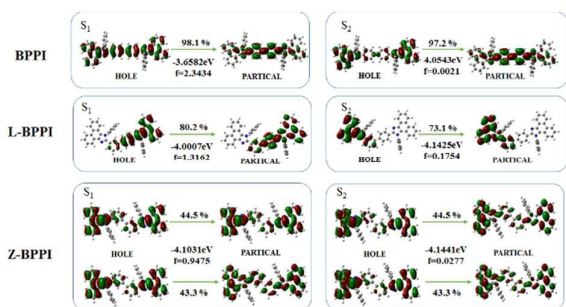


Fig. 1. $S_0 \rightarrow S_1$ and $S_0 \rightarrow S_2$ NTO transition of BPPI, L-BPPI and Z-BPPI

and film states, which is caused by the gradually limited π -electron delocalisation degree with the loss of QY. In fact, the changes are mainly attributed to adjustment in the electronic transitions.

To examine more realistic reasons for the radioactive process in different excited states from *para*-coupling to the *meta*-one, the NTOs and transition dipole moments of the first five singlet and triplet excitations were evaluated, respectively.^{15,18} For simplicity and clarity, Fig. 1 and Fig. 2 show the dominant 'particle'-'hole' contributions and the associated weights for the first two singlet ($S_0 \rightarrow S_n$, $n = 1$ and 2) and two triplet ($S_0 \rightarrow T_n$, $n = 1$ and 2) states of three model isomers, respectively, while Fig. S1-S3 show the other states (S_3 - S_5 and T_3 - T_5), respectively, and Tab. 2 lists their values. In particular, among the five singlet and triplet excited states of the three isomers, almost all 'particles' and 'holes' were localized on the PI and the biphenyl moiety attached to the C2 position, and marginal distribution was observed on the N1-phenyl moiety. These locations indicate that all excited states of the isomers are directed to the C2 direction, significantly more simple than the excited states of the orthotropic systems investigated by Ma, which were directed along the N1 and C2 directions.^{15b,c}

In BPPI, by the excitation of $S_0 \rightarrow S_1$, the 'hole' was primarily located on the entire molecule, while the 'particle' was localized on the biphenyl moiety, with a small fraction on the PI moiety. This distribution implies that S_1 contains a major part of the LE transition of the biphenyl moiety and a minor part of the charge-transfer (CT) transition from PI to the biphenyl unit, corresponding to the aforementioned HLCT. A homologous situation was observed in other excitations such as in the $S_0 \rightarrow S_2$ transition. Its HLCT was primarily composed of CT, with a minor part of LE.^{9d} However, in L-BPPI, two coupling forms (*meta* and *para*) exhibited different excited-state distribution in the molecular framework. For the $S_0 \rightarrow S_1$ excitation, the 'hole' was located on the *para* coupling PI unit and

biphenyl moiety, and the 'particle' was similar to the 'hole', expect for a small difference on the biphenyl moiety. This result implies that S_1 only originates from the *para*-coupling structure, similar to BPPI, but the proportion of the LE transition is higher in its HLCT. A homologous situation was observed in the $S_0 \rightarrow S_2$ transition, but its 'hole' and 'particle' were absent in the *meta*-coupling PI unit. As the oscillator strength of the $S_0 \rightarrow S_2$ excitation is lower than that of the $S_0 \rightarrow S_1$ excitation, it is hypothesised that L-BPPI exhibited radioactive properties with character similar to those of BPPI (as the main radiation process of L-BPPI possibly originates from the *para*-coupling structure). In Z-BPPI, the 'hole' and 'particle' were symmetrically distributed on PI and the biphenyl centre, and every excitation contained two transition configurations at least, which had closer contributions with the only appearance of LE states.

According to the primary viewpoint of HLCT, the increasing proportion of the LE states in the hybrid state was beneficial to the improvement of the PL efficiency because of its Frenkel exciton form,^{15,18,19} but the fluorescence QY decreases in a stepwise manner from BPPI to L-BPPI to Z-BPPI in our previous study.^{9c} A reasonable and detailed explanation for the decrease in the PL efficiencies from *para* to *meta*-coupling has not been provided in previous studies. Herein, by drawing evidence from the data of the three isomers from their NTOs (distribution and strength), two probable reasons were discussed below.

The first and important parameter is the oscillator strength (f) of every excitation in the NTO simulation, which reflects the possibility of this excited-state radiative transition.²⁰ When one of these $S_0 \rightarrow S_n$ excitations is sufficiently greater than the others, the other inter-conversion between different excited states and the non-radiative transition would be limited, typically resulting in high fluorescence efficiency.^{19a} In the three isomers herein, the largest oscillator strength was attributed to the $S_0 \rightarrow S_1$ excitation, indicating that all emissions mainly originate from the S_1 state. However, the $f_{S_0 \rightarrow S_1}$ values gradually decreased from 2.3434 in BPPI to 1.3162 in L-BPPI and to 0.9475 in Z-BPPI, which would result in the PL efficiency of L-BPPI or Z-BPPI being lower than that of BPPI.^{15c,d,9d} The second reason is the energy barriers between the neighbouring excited states and the multiple degenerate states at the same energy level, and the slight difference typically results in a strong orbit coupling, leading to free exciton transformation between the different excited states at room temperature. Consequently, the emission species also change or the number increases with changes in the external environment, such as thermal and electro activation. This frequent internal conversion

Table 2 Calculated energy levels and oscillator strengths of BPPI, L-BPPI and Z-BPPI from NTO

Energy level	BPPI				L-BPPI				Z-BPPI			
	Singlets Energy(eV)	Oscillator Strength	Triplets Energy(eV)	ΔE_{ST}	Singlets Energy(eV)	Oscillator Strength	Triplets Energy(eV)	ΔE_{ST}	Singlets Energy(eV)	Oscillator Strength	Triplets Energy(eV)	ΔE_{ST}
1	-3.6582	2.3434	-2.8552	0.803	-4.0007	1.3162	-3.1081	0.8926	-4.1031	0.9475	-3.1763	0.9268
2	-4.0543	0.0021	-3.0882	0.9661	-4.1425	0.1754	-3.2062	0.9363	-4.1441	0.0277	-3.1977	0.9463
3	-4.1855	0.0456	-3.4087	0.7768	-4.2613	0.2021	-3.5095	0.7518	-4.3185	0.4756	-3.5808	0.7377
4	-4.2657	0.0147	-3.5733	0.6924	-4.3419	0.1554	-3.6563	0.6856	-4.3424	0.0085	-3.6511	0.6913
5	-4.5284	0.0705	-3.7583	0.7701	-4.6120	0.0368	-3.7958	0.8162	-4.6951	0.0038	-3.8072	0.8879

(IC) between the different excited states and transform in the multiple degenerate states would result in the increase in the nonradioactive decay ratio in PL, and the efficiency would become lower than that observed for the $S_1 \rightarrow S_0$ transition with larger oscillator strength.^{9d} In fact, these waning differences in three isomers were obvious, such as in case of $\Delta E_{S_1S_2}$, which decreased from 0.3961 eV in BPPI to 0.1418 eV in L-BPPI to 0.0403 eV in Z-BPPI. Meanwhile, only one preferential conformation was observed in $S_1 \rightarrow S_0$ of BPPI and L-BPPI, while two conformations were observed in Z-BPPI. A prominent feature of broader spectra would be observed in solvatochromic fluorescence measurement as well as in the increase in the proportion of lower-energy-level emissions, which is caused by the lowered energy barriers between the excited states. Sequentially, photo-experiments were conducted to investigate these factors: lower PL efficiency and broader spectra using Z-BPPI.

In addition, the deviations of $S_0 \rightarrow S_1$ clearly increased from *para*-*para* to *meta*-*meta* (Tab. 2), indicative of the gradual widening of the band gap of the three isomers; this result is in agreement with the expected result.^{7, 15d, 11}

On the other hand, a similar distribution was observed for the triplet excited states from NTOs, as shown in Fig. 2 and Fig. S1-3. Most of the excitations exhibited the LE or HLCT state, and the LE proportion increased from BPPI to L-BPPI and Z-BPPI. To investigate the key factors that govern exciton decay and possible reverse intersystem crossing (RISC) conversion in the EL process, the excited-state energy diagrams of three isomers are shown in Fig. 3, including the first five singlet and five triplet excited states. As the coupling changes from *para* to *meta*-coupling, the singlet-triplet energy splitting of S_1T_1 increased, the probability of RISC ($T_1 \rightarrow S_1$)-based cold exciton from thermally activated delayed-fluorescence (TADF) became smaller,²¹ and the EUE would be limited, implying that it was not suitable to construct saturated blue emitters by the tuning of *meta*-coupling in TADF-type materials.

According to the 'hot exciton' mechanism based on the HLCT theory presented by Ma, another type of the RISC process probably occurred in the API block, a novel conversion channel from a high triplet energy level ($T_n, n > 1$) to the suitable singlet (S_m) level, and the two necessary factors must be matched.^{15, 18, 19} First, the singlet-triplet energy splitting ($\Delta E_{S_mT_n}$) between S_m and T_n should be smaller, and the T_n and T_{n-1} states exhibited sufficient separation in energy. As a guarantee, the IC ($T_n \rightarrow T_{n-1}$) rate k_{IC} became too slow to

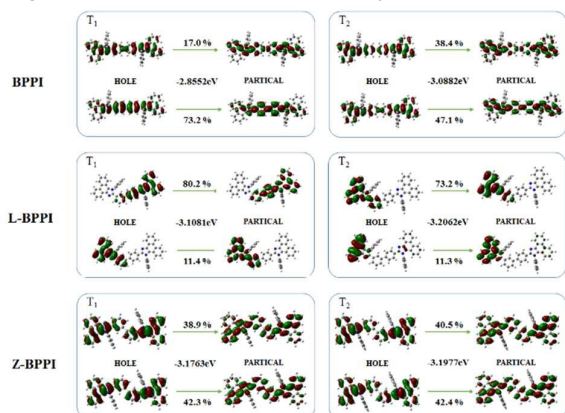


Figure 2. $S_0 \rightarrow T_1$ and $S_0 \rightarrow T_2$ NTO transition of BPPI, L-BPPI and Z-BPPI.

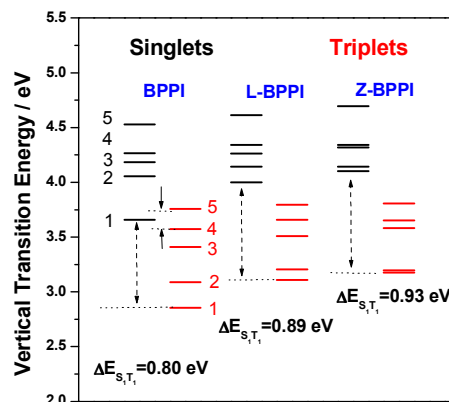


Fig. 3. Energy diagrams of the first five singlet and triplet excited states of BPPI, L-BPPI and Z-BPPI from TD-M06-2X calculations.

compete with the RISC ($T_n \rightarrow S_m$) rate k_{RISC} .^{18c} Second, a similar distribution of excited states and a dominant CT character are very important in S_m and T_n , which could result in the improvement of more loosely bound excitons and lower conversion barriers. In fact, the conversion ratio of the type of excitons became smaller with increasing n value, such as T_2 to S_2 in TPA-NZP^{18b,c} and T_3 to S_1 in PTZ-BZP^{18a}, the higher n value was rare. In L-BPPI and Z-BPPI, the energies of T_5 were clearly lower than those of S_1 , and this 'hot-exciton' process did not occur, albeit some CT character was observed on the T_5 of L-BPPI. The higher energy barriers of S_1T_1 (cold exciton) and S_mT_n (hot exciton) led to the no occurrence of RISC in L-BPPI and Z-BPPI, and their EUEs were not beyond 25%, even if their OLED structures were further optimized. On the other hand, in BPPI, a smaller singlet-triplet energy splitting between S_1 and T_4 (0.0879 eV) or T_5 (0.1001 eV) was observed (Fig. 3), and a similar distribution with some CT character was observed in Fig. S1. Both implied that the excitons conversation might exist in the EL process. However, the n value was very high, and the difference between T_3 and T_4 was not sufficiently large (0.1646 eV, which is far smaller than 1.60 eV of $\Delta E_{T_2T_1}$ in TPA-NZP and 0.76 eV of $\Delta E_{T_3T_2}$ in PTZ-BZP); hence, the RISC process is very limited or does not appear in BPPI EL emission. As a result, the EUE of BPPI is not very high in the device, which barely even extends to 25% after more detail OLED optimization. As compared to classic HLCT materials with EUE values nearing 100%,^{15b,c, 18} the design of the molecular structure of BPPI needs to be improved.

Moreover, a detail was observed in the triplet-energy level: *meta*-tuning clearly exhibited an effect on T_1 and T_2 , while T_3 - T_5 exhibited a marginal change, with large separation between T_3 and T_2 , which were beneficial for the construction of the RISC $T_n \rightarrow S_1$ ($S_2, n \geq 3$) based on the hot-exciton process by the fine tuning of $\Delta E_{S_1-meta, S_1-para}$ (the energy splitting between S_1 -*meta* of the *meta*-isomer and S_1 -*para* of the *para*-one) with the aim of controlling the location of S_1 . The study providing successful evidence for the same was reported by Yang using *anm*TPA-PPi system (from TPA-PPi).^{15a,d}

3.2 Properties of Excited States

For predicting the character of excited states, solvatochromic effects were introduced.^{9d} For this purpose, eight solvents with increasing polarities were used, which had no hydrogen bonds or π - π interactions to the single molecule. With the gradual increase in the polarity of solvent from hexane to acetonitrile, the three isomers exhibited no obvious changes in the absorption spectra, suggesting that the external environment marginally affects the ground state.^{15,22} On the other hand, in the fluorescence spectra, difference was clearly observed.

With the gradual increase in solvent polarity, BPPI exhibited an obvious red-shift from 412 nm in hexane, to 421 nm in THF and to 445 nm in acetonitrile, indicating that BPPI exhibits CT-emitting character in the fluorescent dipole moment of the CT state as evidenced by DFT (Fig. 4A). In L-BPPI, a similar phenomenon was observed, and the location of the main peaks red-shifted from 383 nm in hexane, to 401 nm in THF and to 419 nm in acetonitrile. Although the proportion of CT was limited in L-BPPI NTOs, the transition forms of L-BPPI were nearly located on the *para*-coupling PI unit and biphenyl moiety with a large oscillator strength, and the change trend of L-BPPI spectra resembled the *para*-*para* coupling dimeric one (BPPI). However, in Z-BPPI, which is the *meta*-*meta*

coupling form, the main fluorescent peaks, namely the peak at 366 nm in hexane, 370 nm in THF and 371 nm in acetonitrile, were red-shifted by only 5 nm. At the same time, the intensity of the lower-energy emission band for Z-BPPI was strongly enhanced, and the FWHM became broader. The unchanged main peak originated from the dominant LE character ($f_{S_0-S_1}$, greater than the other excited state in the DFT calculation), and broader spectra were attributed to the increase in the neighbouring excited states, which had an energy level closer to the S_1 state, as evidenced by DFT. The results above proved that *meta*-coupling would result in the main peak moving to the bluer region in API-based materials, but the increased FWHM would affect the purity of the emission colour. Hence, some more attention should be paid to the process of tuning.

The dipole moment of the S_1 state can be estimated from the slope of the plot of the Stokes shifts ($\nu_a - \nu_f$) against the solvent parameters $f(\epsilon, n)$ (or orientation polarisability) according to the Lippert–Mataga equation shown in Equation S1 (for details, see Supporting Information).^{9,15} The fitted results reflect a non-linear relationship between the Stokes shift and solvent polarity, as shown

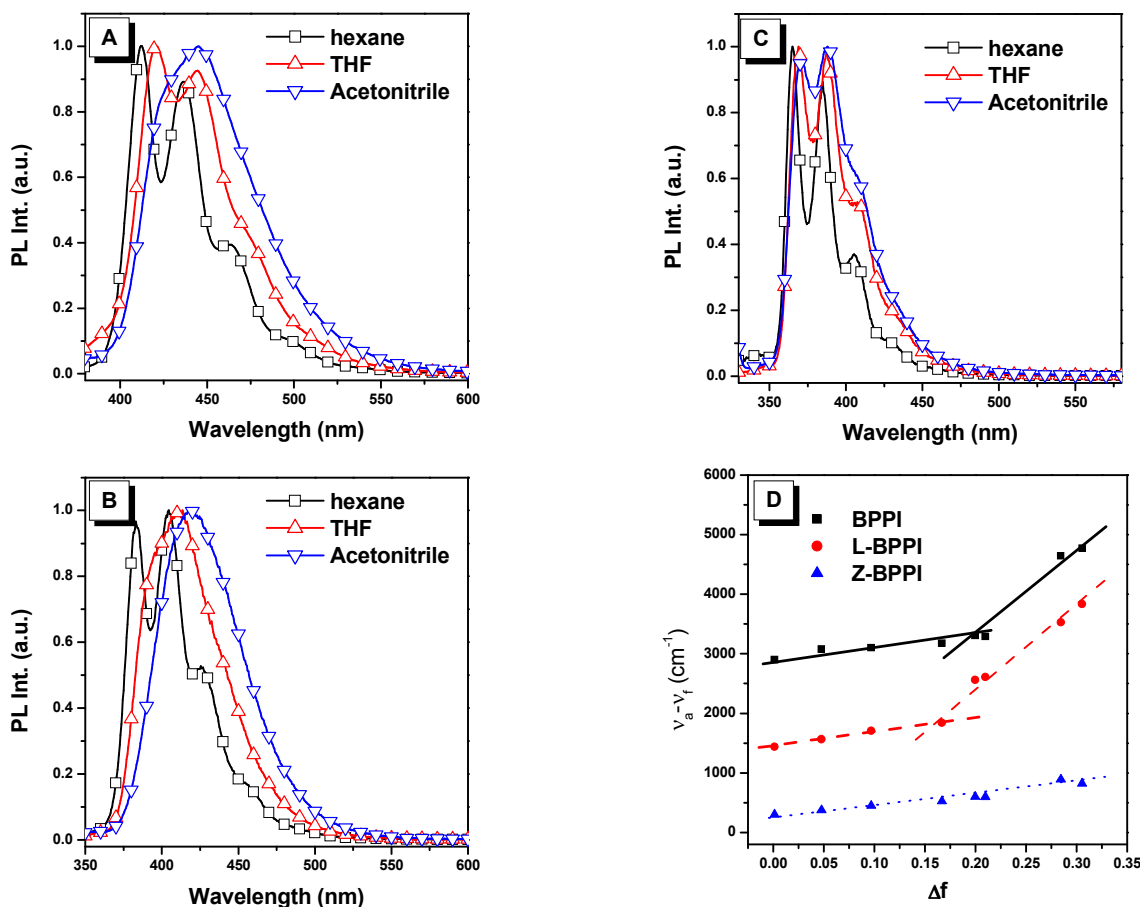


Fig. 4. Solvatochromic fluorescence in solvents with increased solvent polarities: (A) BPPI, (B) L-BPPI and (C) Z-BPPI; (D) Linear correlation of orientation polarization (f) of the solvent media with the Stokes shift ($\nu_a - \nu_f$) for the three isomers.

in Fig. 4D. Two independent slopes of the fitted line suggest the existence of two different excited states in BPPI and L-BPPI. In highly polar solvents, their dipole moments (μ_e) were calculated to be 20.7 D for BPPI and 19.8 D for L-BPPI (slope = 14721, $r = 0.99$ for BPPI and slope = 13506, $r = 0.99$ for L-BPPI), while in less polar solvents, their values were 7.80 D (slope = 2093, $r = 0.90$) for BPPI and 7.73 D (slope = 2052, $r = 0.95$) for L-BPPI. A μ_e of 7.80 D (or 7.73D) was attributed to the usual excited state, which was a class LE-like state. A large μ_e value of 20.7 D (or 19.8 D) should be treated as a CT-like state, whose value was very close to a typical CT molecule DMABN with a μ_e of 23 D.^{23a} The fluorescent solvatochromic experiments and non-linear relationship between the Stokes shift and solvent polarity indicated that the two isomers exhibit inter-crossed LE and CT excited states with HLCT states similar to TPA-NZB.^{18b} On the other hand, Z-BPPI exhibited simple linearity (slope = 307, $r = 0.96$), which represented a single emitting species with a μ_e of 7.0 D. This value was similar to that of typical LE emitters, implying that the S1 emissive state of Z-BPPI contained a marginal part of the CT component.^{23b} All results obtained from solvatochromic effects were consistent to the hypothesis in DFT.

3.3 Electroluminescence Properties

Based on a previous study, three comparable devices were fabricated as ITO/m-M-MoO_x(30 nm)/NPB (20 nm)/BPPI or L-BPPI or Z-BPPI (30 nm)/3TPyMBi (20 nm)/Mg:Ag (10:1 by weight, 100 nm) for investigating their EL properties, as shown Fig. 5A, in which m-M, MoO_x, NPB and 3TPyMBi were used as the carrier-modified layers with respect to their appropriate energy levels.²⁴

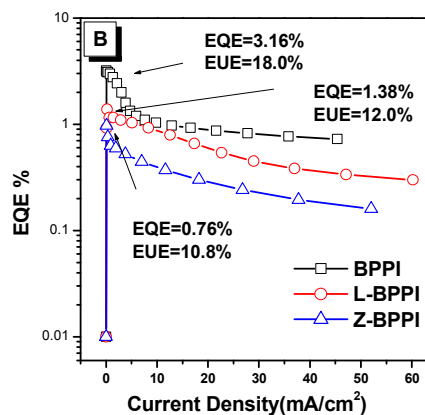
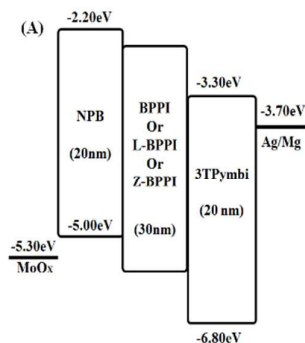


Fig. 5. (A) EL structure of the device; (B) the EQE versus current density curve in device.

Table 3. Summary of the device performance of BPPI, L-BPPI and Z-BPPI.

Device	CIE ^[a]	Vol ^[b]	LE ^[c]	PE ^[d]	L ^[e]	EQE ^[f]	EUE ^[g]
BPPI	0.15,0.13	3.5	3.52	3.16	363	3.18	18.7
L-BPPI	0.15,0.10	5	0.97	0.61	452	1.38	11.5
Z-BPPI	0.17,0.11	5	0.56	0.35	709	0.76	10.8

[a] (x, y), Recorded at 9 V. [b] Turn-on voltage, [V], ($L > 1 \text{ cdm}^{-2}$). [c] Maximum values of luminance, (LE_{max}), [cdA^{-1}]. [d] Power efficiency, (PE_{max}), [lmW^{-1}]. [e] Maximum brightness, (L_{max}), [cdm^{-2}]. [f] Maximum external quantum efficiency, (EQE_{max}), (%). [g] Maximum exciton utilising efficiency, (EUE_{max}), (%).

The EL spectra of three emitters exhibited deep-blue emission with CIE coordinates of (0.15, 0.13) for BPPI, (0.15, 0.10) for L-BPPI and (0.17, 0.11) for Z-BPPI, respectively (shown in Fig. S4), the values of which were in good agreement with the requirement of the NTSC standard blue CIE coordinate of $(x + y) < 0.3$.⁶ A specific situation occurred in Z-BPPI, which exhibited the most intense blue emission in the three isomers, but its CP of the EL emissions was not best. The increasing intensity of the lower-energy emission was enhanced to the main emission state by the reaction of electric field in EL process, and unexpected results were appeared, such as the main-peak red-shift and the broader FWHM, which were all in agreement with the results obtained from DFT and spectral measurements.

Although all devices exhibited low luminescence, a basic trend was identified on the basis of the data listed in Tab. 3. In the same measurement, BPPI-based devices exhibited better performance with a maximum current efficiency of $\sim 3.52 \text{ cdA}^{-1}$, a maximum power efficiency of $\sim 3.16 \text{ lmW}^{-1}$ and a maximum EQE (η_{ext}) of $\sim 3.18\%$. According to the relation equation between EQE and EUE shown in Equation S2,^{9d,15} its EUE value was estimated to be 18.0% from the solid-state efficiency ($\sim 85\%$). L-BPPI and Z-BPPI exhibited

relatively similar performances with maximum current efficiencies of $\sim 0.97 \text{ cdA}^{-1}$ and 0.56 cdA^{-1} , respectively, with corresponding maximum EQEs of $\sim 1.38\%$ and 0.76% . The efficiencies of L-BPPI and Z-BPPI were only 57% and 35% in the film state, and their corresponding EUE values were estimated to be only $\sim 12.0\%$ and 10.8% (Fig. 5B).

The EUEs of the three isomers did not exceed the 25% limit of spin statistics, implying that the RISC process may not be excited in the EL process; this result was consistent with the discussion in DFT analysis about singlet and triplet conversion. To the three isomers, these EL emissions originated from their pure fluorescence components without the RISC process, and the EL efficiency was decided by their PL yield as described in Equation S2. This result implies that *meta*-tuning barely realized improvement in EL, unless some special excited states form or a conversion channel appeared, such as the RISC process among others.

4. Conclusions

In summary, three isomers with a dimeric phenanthroimidazole framework were chosen as examples to investigate the effect of *meta*-coupling on their excited state in deep-blue emitters. By the combination of detailed photophysical data, device performance, and DFT calculations, some valuable information was obtained. In particular, the relationship between some key parameters in calculations and their PL or EL properties was confirmed, which could effectively reduce the issues related to synthesis and characterisation by using prior computer simulations. By comparing the isomers, the tuning effect from *para* to *meta*-coupling was listed below, which was beneficial for the further optimisation of the molecular structure for high-performance deep-blue emitters with good fluorescence quantum yields, exciton utilising efficiency and colour purity.

- (1) The degree of conjugation would be limited by this *meta*-coupling, and the difference between S_1 and S_0 increased with increasing band gap; hence, the main fluorescence peak showed a blue-shift.
- (2) The oscillator strength of S_1 decreased in the *meta*-isomer, and the energy barriers between the neighbouring excited states were lower than those in the *para*-isomer, which all contribute to the decrease in photoluminescence efficiency. This frequent internal conversion between different excited states caused by the slight energy barriers could lead to instability in the excited states, which could be easily disturbed by the external environment; hence, FWHM was affected.
- (3) The energy splitting of S_1T_1 became greater, and the cold-exciton process was inhibited, which was not an advisable strategy for the construction of TADF-type materials. *Meta*-coupling obviously affected T_1 and T_2 , and their separation became small, but the higher triplet changed marginally. If $S_{1\text{-meta}}$ (or $S_{2\text{-meta}}$) and $T_{n\text{-meta}}$ ($n \geq 3$) could meet the requirements of the hot-exciton process condition, RISC could occur to enhance EL performance; hence, the difference between $S_{1\text{-meta}}$ and $S_{1\text{-para}}$ was important.

On balance, the strategy for tuning *meta*-coupling by the construction of a *meta*-isomer is important for controlling the

compound emission colour in the field of organic photo-electro materials, particularly for the design of blue emitters. The blue-shift of the main fluorescence peak and the loss of photoluminescence efficiency are two inevitable factors; hence, special conversion (such as RISC) between excited states is a key factor for the maintenance or improvement of the EL efficiency (EQE or EUE), while this construction absolutely depends on the chemical structures of substituted groups at both ends of the (*meta*- or *para*-) coupling position. Not all materials are suitable for the tuning of *meta*-coupling, with the exception that they have a suitable energy level between $S_{n\text{-meta}}$ and $S_{n\text{-para}}$ ($n=1$ or 2). The construction of a donor-acceptor system is preferable for more valuable *meta*-tuning for the preparation of non-doped deep-blue electroluminescent materials based on APIs, following our analysis above.

Acknowledgements

This work is financially supported by National Science Foundation of China (51203091, 60907013 and 61377026), Liaoning Province Doctor Start-up Fund (Grant No. 20131084), China Postdoctoral Science Foundation Grant (2014M562213, 2015T80919), Science and Technology Plan of Shenzhen (JCYJ20140425170011516), and Natural Science Fund of Guangdong Province (2014A030313659).

Notes and references

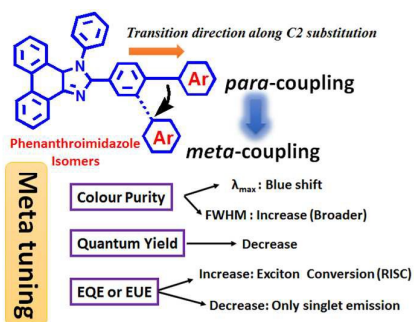
- (a) M. T. Lee, H. H. Chen, C. H. Liao, C. H. Tsai and C. H. Chen, *Appl. Phys. Lett.*, 2004, **85**, 3301; (b) Y. Wei and C. T. Chen, *J. Am. Chem. Soc.*, 2007, **129**, 7478.
- (a) H. H. Chou, Y. H. Chen, H. P. Hsu, W. H. Chang, Y. H. Chen and C. H. Cheng, *Adv. Mater.*, 2012, **24**, 5867; (b) C. L. Liu, C. J. Zheng, X. K. Liu, Z. Chen, J. P. Yang, F. Li, X. M. Oua and X. H. Zhang, *J. Mater. Chem. C*, 2015, **3**, 1068.
- (a) A. Kraft, A. C. Grimsdale and A. B. Holmes, *Angew. Chem. Int. Ed.*, 1998, **37**, 402; (b) M. T. Lee, C. H. Liao, C. H. Tsai and C. H. Chen, *Adv. Mater.*, 2005, **17**, 2493.
- (a) Y. J. Tung, T. Nago, M. Hack, J. Brown, N. Koide, Y. Nagara, Y. Kato and H. Ito, *SID 2004 Technical Digest*, 2004, **35**, 48; (b) H. Huang, Y. X. Wang, S. Q. Zhuang, X. Yang, L. Wang and C. L. Yang, *J. Phys. Chem. C*, 2012, **116**, 19458.
- (a) M. Zhu and C. Yang, *Chem. Soc. Rev.*, 2013, **42**, 4963; (b) C. C. Wu, Y. T. Lin, K. T. Wong, R. T. Chen and Y. Y. Chien, *Adv. Mater.*, 2004, **16**, 61.
- (a) S. Tang, M. R. Liu, P. Lu, H. Xia, M. Li, Z. Q. Xie, F. Z. Shen, C. Gu, H. Wang, B. Yang and Y. G. Ma, *Adv. Funct. Mater.*, 2007, **17**, 2869; (b) N. T. Gurin, K. V. Paksyutov, M. A. Terent'ev, A. V. Shirokov, *Tech. Phys.*, 2012, **57**, 308; (c) S. Difley, D. Beljonne, T. V. Voorhis, *J. Am. Chem. Soc.*, 2008, **130**, 3420.
- (a) J. Huang, R. Tang, T. Zhang, Q. Li, G. Yu, S. Xie, Y. Liu, S. Ye, J. Qin and Z. Li, *Chem. Eur. J.*, 2014, **20**, 5317; (b) J. Huang, N. Sun, J. Yang, R. Tang, Q. Li, D. Ma, J. Qin and Z. Li, *J. Mater. Chem. C*, 2012, **22**, 12001; (c) J. Huang, N. Sun, Y. Dong, R. Tang, P. Lu, P. Cai, Q. Li, D. Ma, J. Qin and Z. Li, *Adv. Funct. Mater.*, 2013, **23**, 2329.
- (a) C. J. Kuo, T. Y. Li, C. C. Lien, C. H. Liu, F. I. Wu and M. J. Huang, *J. Mater. Chem.*, 2009, **19**, 1865; (b) C. H. Cheng, C. H. Liu and F. I. Wu, 2010, *U.S. Patent* No. 20100253208.
- (a) Z. M. Wang, P. Lu, S. M. Chen, Z. Gao, F. Z. Shen, W. S. Zhang, Y. X. Xu, H. S. Kwok and Ma Y. G. *J. Mater. Chem.*, 2011, **21**, 5451; (b) Z. M. Wang, X. H. Song, Z. Gao, D. W. Yu, X. J. Zhang, P. Lu, F. Z. Shen and Y. G. Ma, *RSC Adv.*, 2012, **2**, 9635. (c) Z. M.

- Wang, Y. Feng, H. Li, Z. Gao, X. J. Zhang, P. Lu, P. Chen, Y. Ma and S. Liu, *Phys. Chem. Chem. Phys.*, 2014, **16**, 10837; (d) Z. M. Wang, Y. Feng, S. T. Zhang, Y. Gao, Z. Gao, Y. M. Chen, X. J. Zhang, P. Lu, B. Yang, P. Chen, Y. G. Ma and S. Y. Liu, *Phys. Chem. Chem. Phys.*, 2014, **16**, 20772.
- 10 (a) Z. Gao, G. Cheng, F. Z. Shen, S. T. Zhang, Y. Zhang, P. Lu and Y. G. Ma, *Laser Photon. Rev.*, 2014, **8**, L6; (b) Z. Gao, Y. L. Liu, Z. M. Wang, F. Z. Shen, H. Liu, G. N. Sun, L. Yao, Y. Lv, P. Lu and Y. G. Ma, *Chem. Eur. J.*, 2013, **19**, 2602; (c) Z. Gao, Z. M. Wang, T. Shan, Y. L. Liu, F. Z. Shen, Y. Y. Pan, H. H. Zhang, X. He, P. Lu, B. Yang and Y. G. Ma, *Org. Electro.*, 2014, **15**, 2667.
- 11 (a) K. Wang, S. P. Wang, J. B. Wei, S. Y. Chen, D. Liu, Y. Liu and Y. Wang, *J. Mater. Chem. C*, 2014, **2**, 6817; (b) K. Wang, S. P. Wang, J. P. Wei, Y. Miao, Y. Liu and Y. Wang, *Org. Electro.*, 2014, **15**, 3211; (c) D. Liu, M. X. Du, D. Chen, K. Q. Ye, Z. L. Zhang, Y. Liu, and Yue Wang, *J. Mater. Chem. C*, 2015, **3**, 4394.
- 12 (a) Y. Zhang, J. H. Wang, J. Zheng and D. Li, *Chem. Commun.*, 2015, **51**, 6350; (b) Y. Yuan, J. X. Chen, W. C. Chen, S. F. Ni, H. X. Wei, J. Ye, F. Lung Wong, Z. W. Zhou, Q. X. Tong and C. S. Lee, *Org. Electro.*, 2015, **18**, 61; (c) W. C. Chen, G. F. Wu, Y. Yuan, H. X. Wei, F. L. Wong, Q. X. Tong and C. S. Lee, *RSC Adv.*, 2015, **5**, 18067.
- 13 (a) H. Huang, Y. X. Wang, S. Q. Zhuang, X. Yang, L. Wang and C. L. Yang, *J. Phys. Chem. C*, 2012, **116**, 19458; (b) S. Zhuang, R. Shanguan, H. Huang, G. Tua, L. Wang and X. Zhu, *Dyes Pigments*, 2014, **101**, 93; (c) B. Wang, G. Y. Mu, J. H. Tan, Z. H. Lei, J. J. Jin and L. Wang, *J. Mater. Chem. C*, 2015, **3**, 7709.
- 14 (a) X. Y. Zhang, J. Lin, X. H. Ouyang, Y. Liu, X. Y. Liu and Z. Y. Ge, *J. Photochem. Photobiol. A*, 2013, **268**, 37; (b) D. Kumar, K. R. J. Thomas, C. Lin and J. Jou, *Chem. Asian J.*, 2013, **8**, 2111; (c) R. Misra, T. Jadhav, B. Dhokale and S. M. Mobin, *Chem. Commun.*, 2014, **50**, 9076.
- 15 (a) W. J. Li, D. D. Liu, F. Z. Shen, D. G. Ma, Z. M. Wang, T. Feng, Y. X. Xu, B. Yang and Y. G. Ma, *Adv. Funct. Mater.* 2012, **22**, 2797; (b) S. T. Zhang, W. J. Li, L. Yao, Y. Y. Pan, B. Yang and Y. G. Ma, *Chem. Commun.* 2013, **49**, 11302; (c) S. T. Zhang, L. Yao, Q. M. Peng, W. J. Li, Y. Y. Pan, R. Xiao, Y. Gao, C. Gu, Z. M. Wang, P. Lu, F. Li, S. J. Su, B. Yang and Y. G. Ma, *Adv. Funct. Mater.*, 2015, **25**, 1755; (d) H. C. Liu, Q. Bai, L. Yao, H. Y. Zhang, H. Xu, S. T. Zhang, W. J. Li, Y. Gao, J. Y. Li, P. Lu, H. Y. Wang, B. Yang and Y. G. Ma, *Chem. Sci.*, 2015, **6**, 3797.
- 16 (a) J. Y. Xiang, Xi. L. Cai, X. D. Lou, G. X. Feng, X. H. Min, W. W. Luo, B. R. He, C. C. Goh, L. G. Ng, J. Zhou, Z. J. Zhao, B. Liu and B. Z. Tang, *Appl. Mater. Interfaces*, 2015, **7**, 14965; (b) X. H. Ouyang, X. L. Li, L. Ai, D. B. Mi, Z. Y. Ge and S. J. Su, *ACS Appl. Mater. Interfaces*, 2015, **7**, 7869; (c) W. Qin, Z. Y. Yang, Y. B. Jiang, J. W. Y. Lam, G. D. Liang, H. S. Kwok and B. Z. Tang, *Chem. Mater.*, 2015, **27**, 3892.
- 17 (a) B. Yang, S. K. Kim, H. Xu, Y. I. Park, H. Zhang, C. Gu, F. Z. Shen, C. L. Wang, D. D. Liu, X. D. Liu, M. Hanif, S. Tang, W. J. Li, F. Li, J. C. Shen, J. W. Park and Y. G. Ma, *Chem. Phys. Chem.* 2008, **9**, 2601; (b) S. K. Kim, B. Yang, Y. G. Ma, J. H. Lee and J. W. Park, *J. Mater. Chem.* 2008, **18**, 3376; (c) S. K. Kim, B. Yang, Y. I. Park, Y. G. Ma, J. Y. Lee, H. J. Kim and J. Park, *Org. Electron.* 2009, **10**, 822.
- 18 (a) L. Yao, S. T. Zhang, R. Wang, W. J. Li, F. Z. Shen, B. Yang and Y. G. Ma, *Angew. Chem. Int. Ed.* 2014, **53**, 2119; (b) W. J. Li, Y. Y. Pan, R. Xiao, Q. M. Peng, S. T. Zhang, D. G. Ma, F. Li, F. Z. Shen, Y. H. Wang, B. Yang and Y. G. Ma, *Adv. Funct. Mater.*, 2013, **24**, 1609; (c) Y. Pan, W. Li, S. Zhang, L. Yao, C. Gu1, H. Xu, B. Yang and Y. Ma, *Adv. Opt. Mater.*, 2014, **2**, 510.
- 19 L. Yao, B. Yang, Y. G. Ma, *Sci. China Chem.*, 2013, **43**, 1457.
- 20 (a) M. J. Frisch, et al. Gaussian 09, revision A.02, Gaussian, Inc., Wallingford CT, 2009; (b) T. Yanai, D. P. Tew, N. C. Handy, *Chem. Phys. Lett.* 2004, **393**, 51; (c) T. Yanai, R. J. Harrison, N. C. Handy, *Mol. Phys.* 2005, **103**, 413; (c) Lippert, et. al. In *Advances in Molecular Spectroscopy*; Mangini, A., 95 Ed. Pergamon Press: Oxford, 1962; p 443
- 21 (a) K. Goushi, K. Yoshida, K. Sato, and C. Adachi, *Nature Photonics*, 2012, **6**, 253; (b) Q. Zhang, B. Li, S. Huang, H. Nomura, H. Tanaka, C. Adachi. *Nature Photonics*, 2014, **8**, 326; (c) Y. Tao, K. Yuan, T. Chen, P. Xu, H. Li, R. Chen, C. Zheng, L. Zhang, W. Huang, *Adv. Mater.*, 2014, **17**, 7931.
- 22 (a) Z. M. Wang, X. H. Song, L. L. Ma, Y. Feng, C. Gu, X. J. Zhang, P. Lu and Y. G. Ma, *New J. Chem.*, 2013, **37**, 2440; (b) Z. Wang, P. Lu, S. Xue, C. Gu, Y. Lv., Q. Zhu, H. Wang and Y. Ma, *Dyes Pigments*, 2011, **91**, 356.
- 23 a) Z. R. Grabowski, K. Rotkiewicz, W. Rettig, *Chem. Rev.*, 2003, **103**, 3899; b) Z. R. Grabowski, Rotkiewicz, *E. Acta Phys. Polon.* 1978, **54A**, 767.
- 24 (a) C. C. Wu, Y. T. Lin, K. T. Wong, R. T. Chen and Y. Y. Chien, *Adv. Mater.*, 2004, **16**, 61-65; (b) P. Chen, W. F. Xie, J. Li, T. Guan, Y. Duan, Y. Zhao, S. Y. Liu and C.S. Ma, *Appl. Phys. Lett.*, 2007, **91**, 023505; (c) P. Chen, Q. Xue, W. F. Xie, Y. Duan, G. H. Xie, Y. Zhao, J. Y. Hou, S. Y. Liu, L. Y. Zhang and B. Li, *Appl. Phys. Lett.*, 2008, **93**, 153508; (d) P. Chen, Q. Xue, W. F. Xie, Y. Duan, G. H. Xie, Y. Zhao, J. Y. Hou, S. Y. Liu, L. Y. Zhang and B. Li, *Appl. Phys. Lett.*, 2009, **95**, 123307.

Graphical Abstract

Effect of Meta Coupling on Colour Purity, Quantum Yield, and Excitons Utilizing Efficiency in Deep-Blue Emitters from Phenanthroimidazole Isomers

Zhiming Wang, Xueying Li, Wanyu Zhang, Shitong Zhang, Hui Li, Zhenqiang Yu, Yanming Chen, Ping Lu and Ping Chen



Three isomers were employed to investigate the essential reason of the *meta*-tuning effect on their PL and EL properties.